Electronic Supplementary Material (ESI) for New Journal of Chemistry.

Supplementary Information

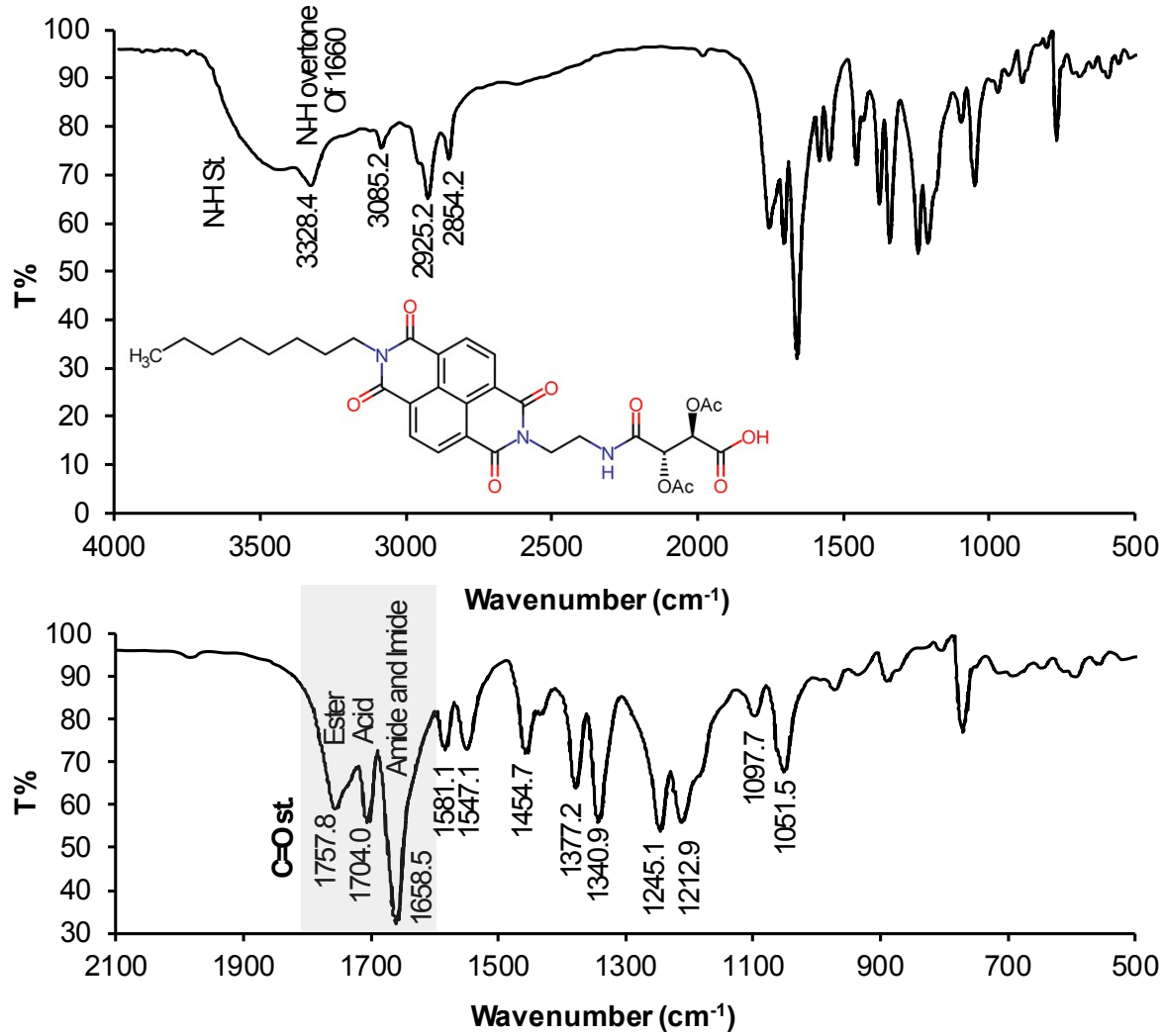

Fig. S1 FT-IR spectra of NDI-TA1 powder.

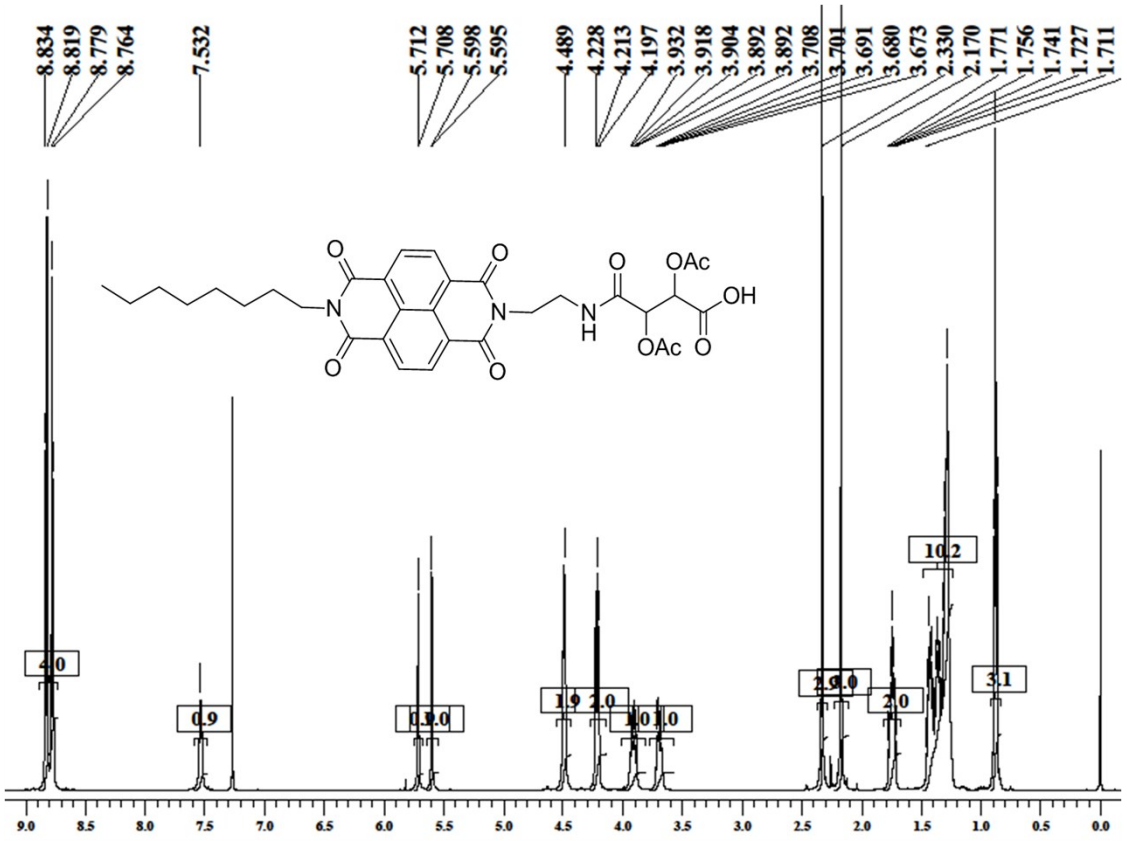

Fig. S2 [1]H NMR spectra of compound NDI-TA1.

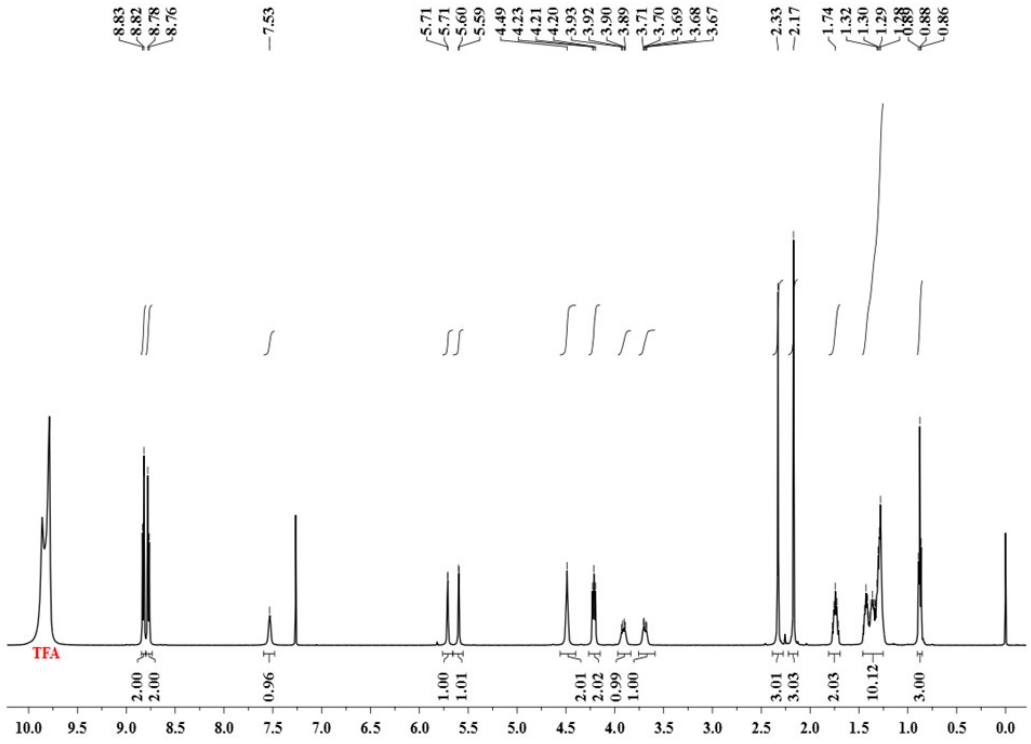

Fig. S3 [1]H NMR spectra of compound NDI-TA1 (TFA-*d*).

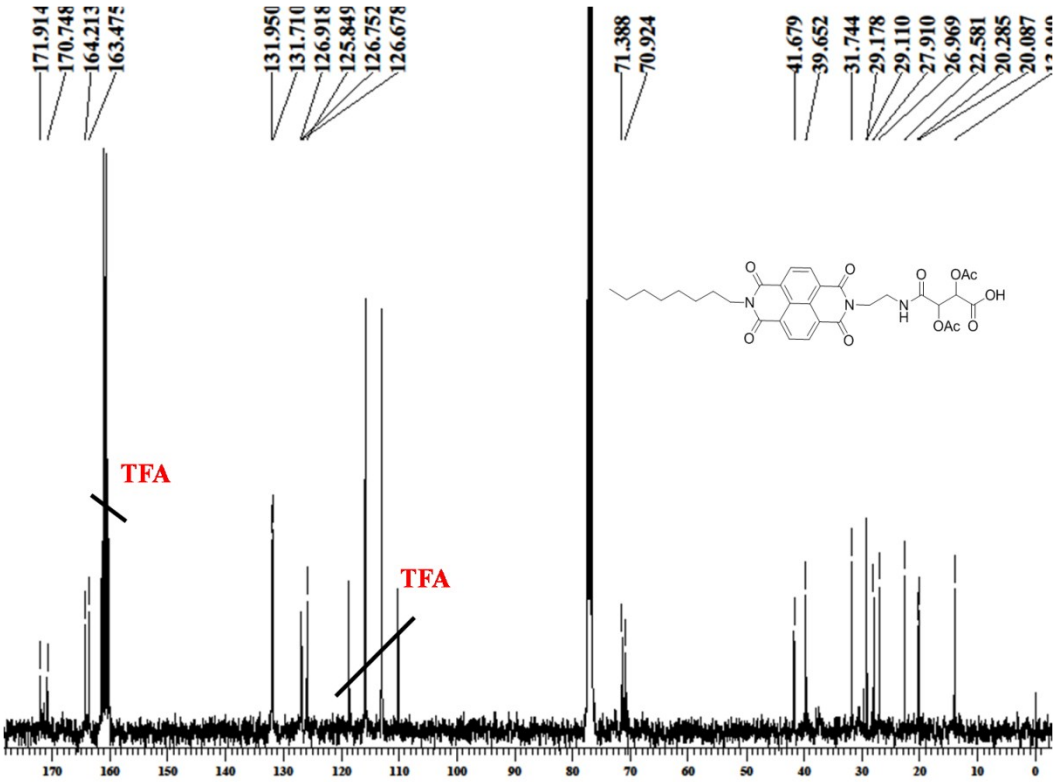

Fig. S4 ^{13}C NMR spectra of compound NDI-TA1.

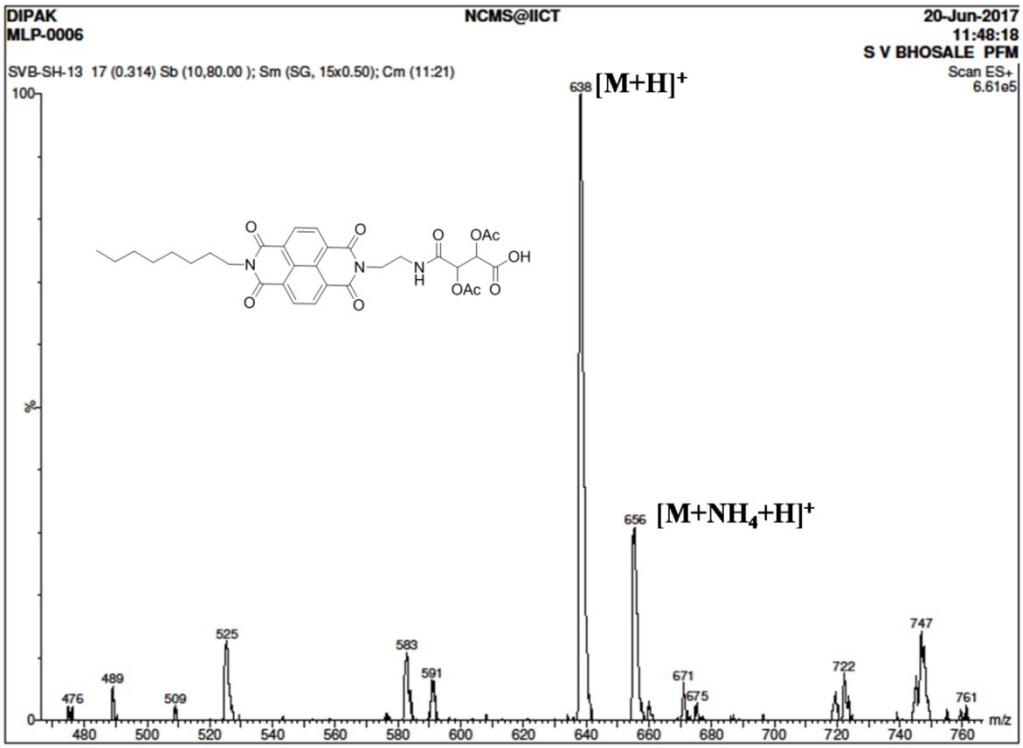

Fig. S5 ESI mass spectra of compound NDI-TA1.

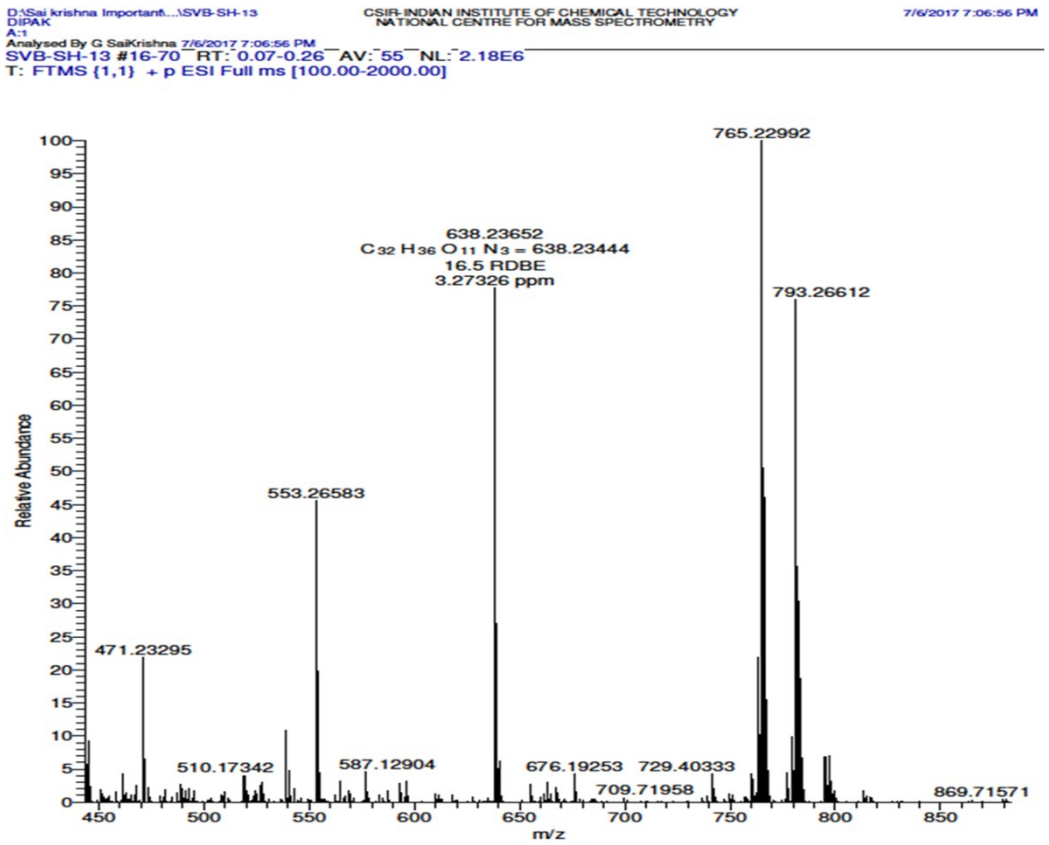

Fig. S6 HRMS spectra of compound NDI-TA1.

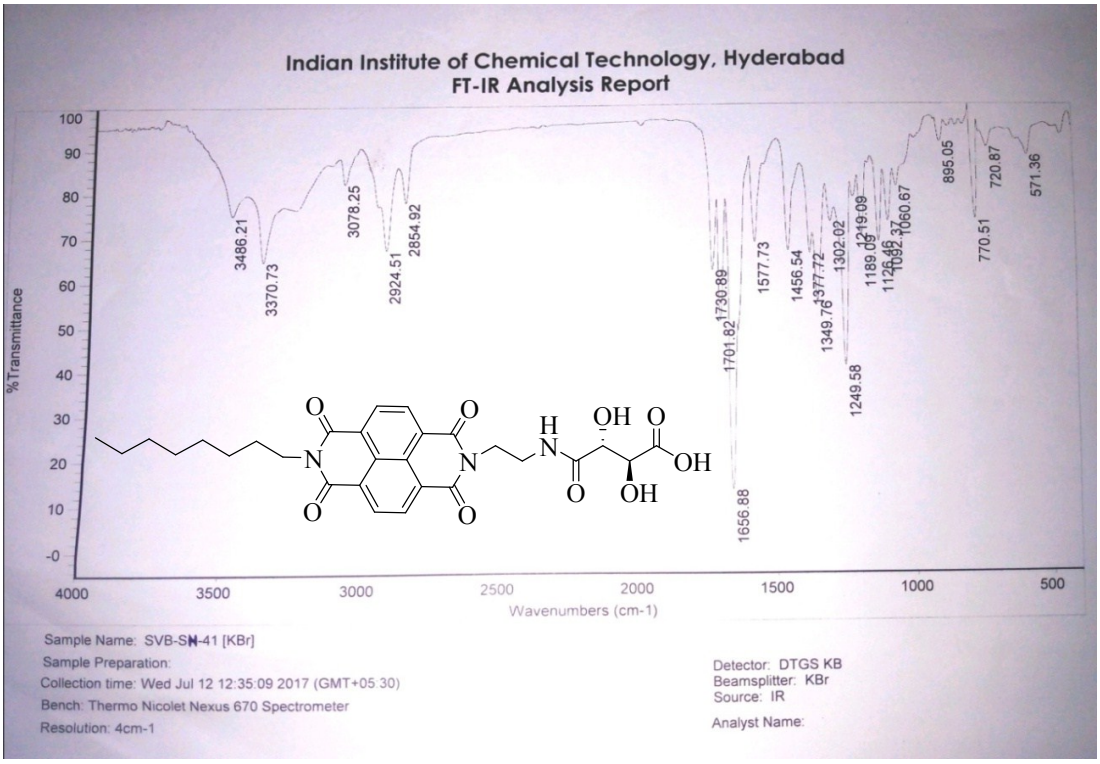

Fig.S7 FT-IR spectra of compound NDI-TA2.

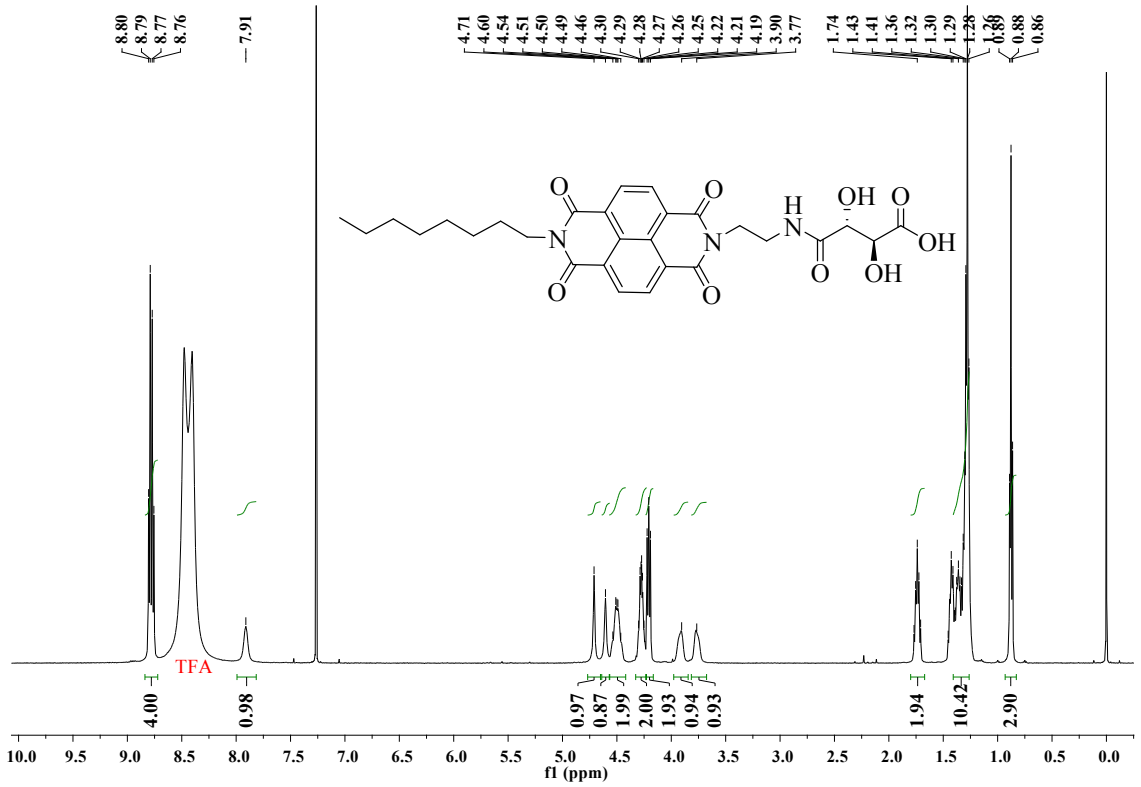

Fig. S8 [1]H NMR spectra of compound NDI-TA2.

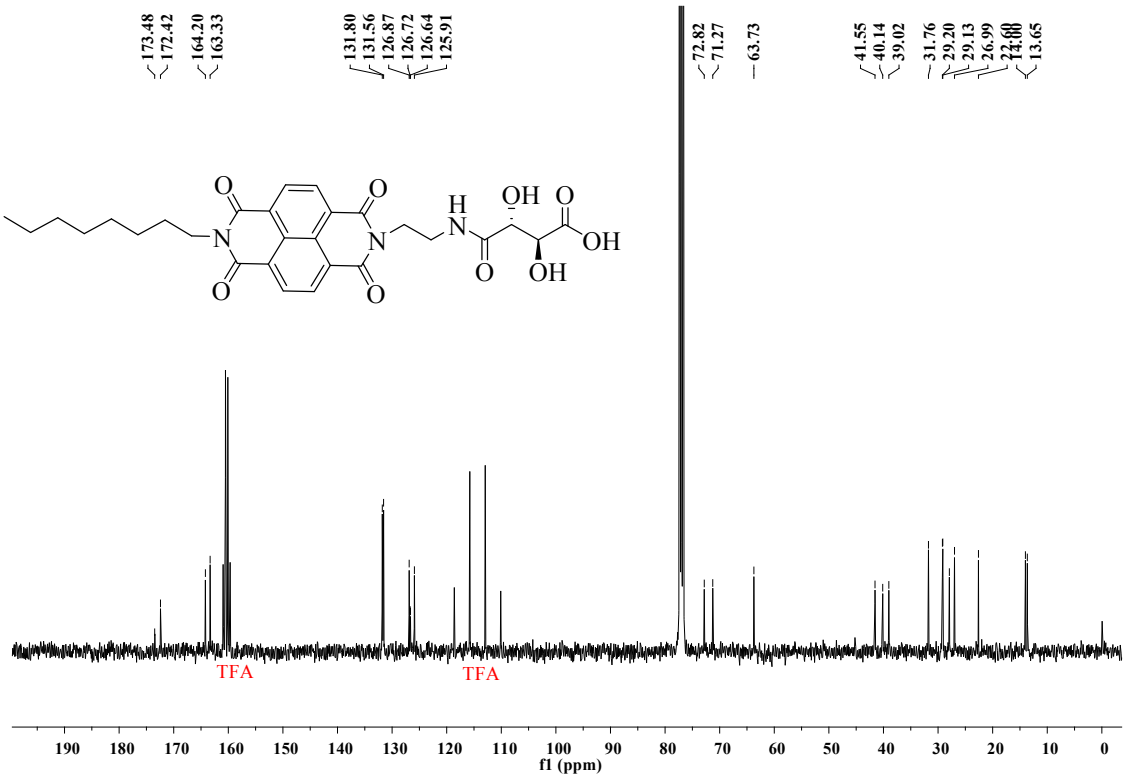

Fig. S9 [13]C NMR spectra of compound NDI-TA2.

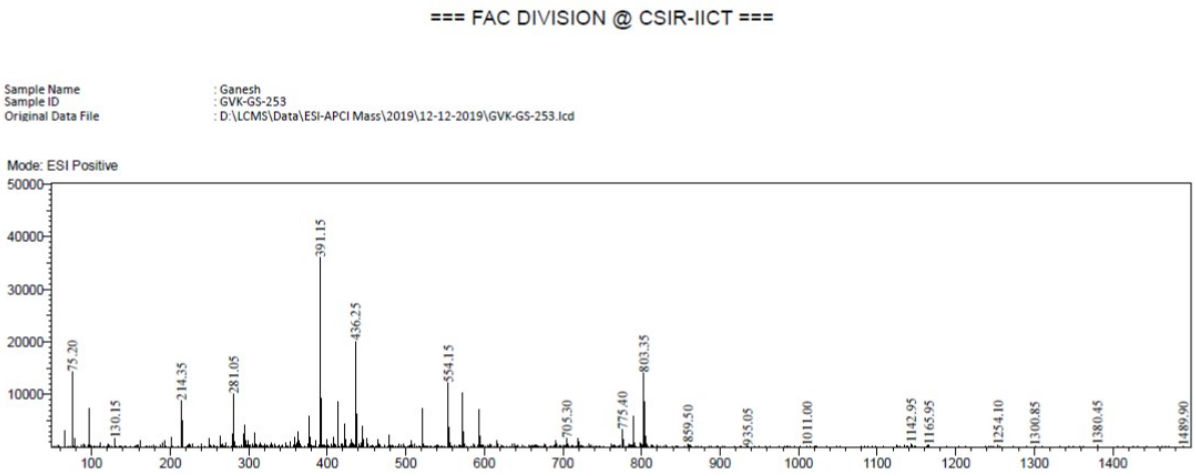

Fig. S10 ESI mass spectrum of compound NDI-TA2.

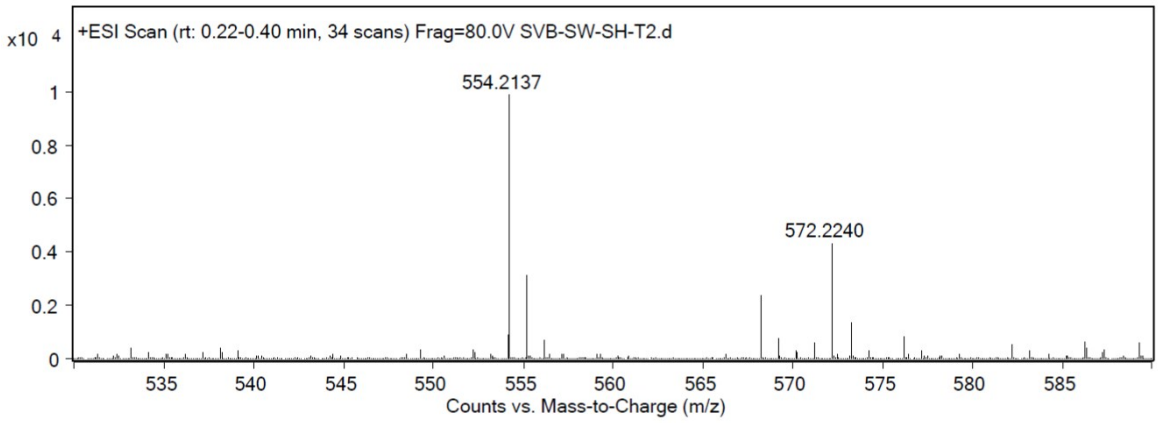

Peak List

m/z	Abund
59.0494	233563.31

Formula Calculator Element Limits

Element	Min	Max
C	0	30
H	0	60
O	0	9
N	0	5
S	0	2
F	0	0
Cl	0	1

Formula Calculator Results

Formula	Best	Mass	Tgt Mass	Diff (ppm)	Ion Species	Score
C28 H32 N3 O9	True	554.2142	554.2139	-0.58	C28 H32 N3 O9	99.46

Fig. S11 ESI HRMS spectrum of compound NDI-TA2.

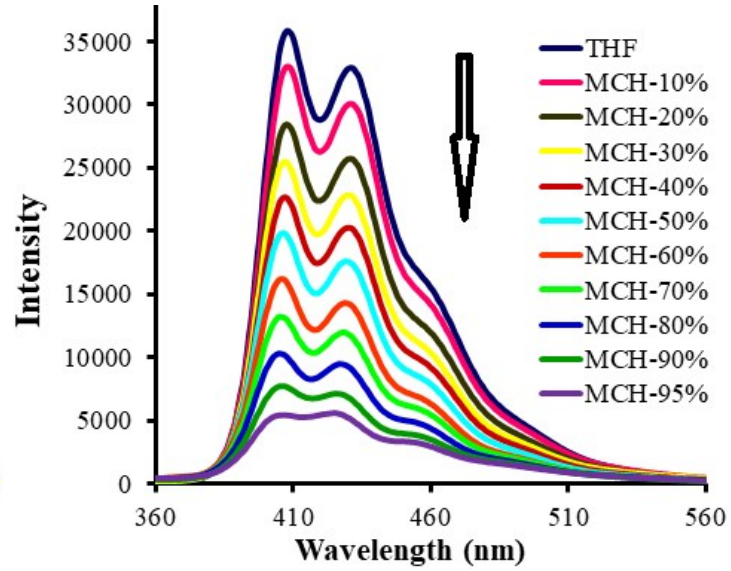

Fig.S12 Emission spectra (λ_{ex} = 350 nm) of NDI-TA2 in THF solution (1×10^{-5} M) while titration with MCH (0 – 95% *v*/*v*). It can be clearly seen that upon gradual addition with increase in volume ratios fluorescence emission is diminishing which is related to ACQ effect.

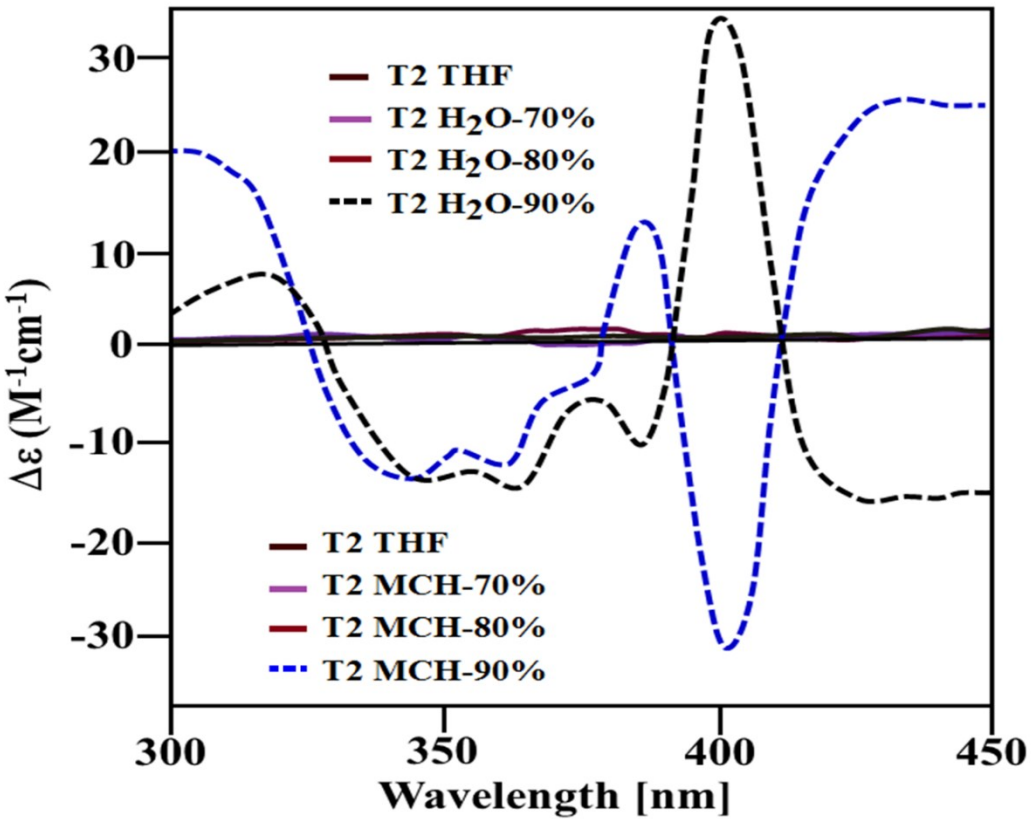

Fig. S13 The circular dichroism (CD) spectra of NDI-TA2 at various THF/MCH and THF/water volume ratios. THF/MCH v/v 10:90 (dotted blue curve) and THF/Water v/v 10:90 (dotted black curve).

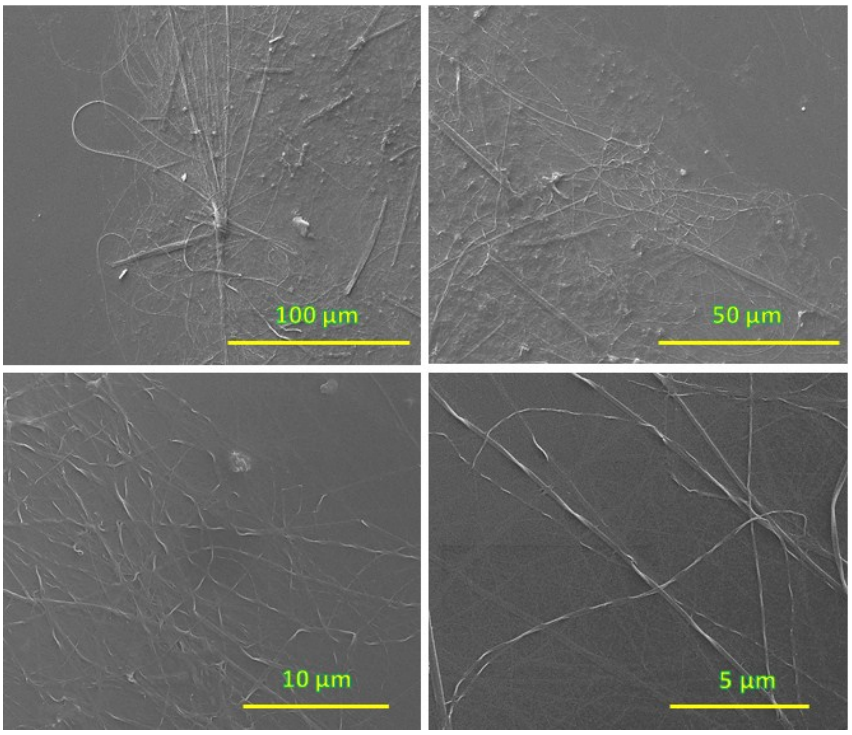

Fig. S14 SEM micrograph of NDI-TA1 self-assembled solid deposited from THF:MCH 10:90, images with various sizes (wide view).

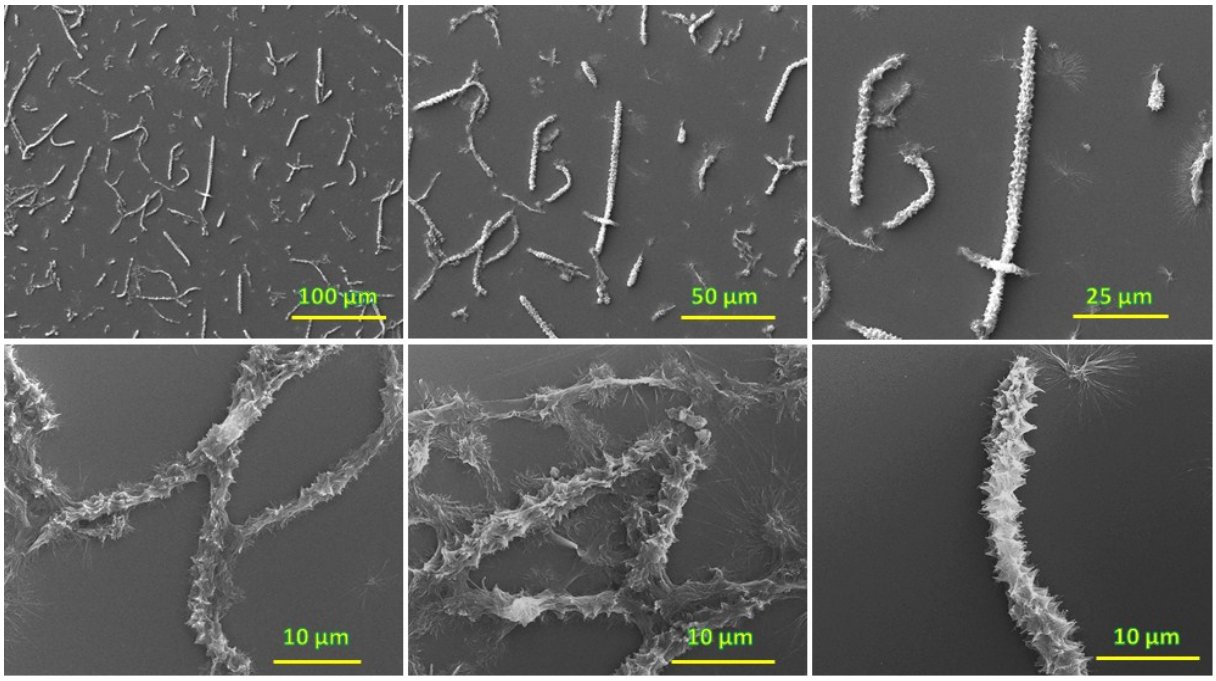

Fig. S15 SEM micrograph of NDI-TA1 self-assembled solid deposited from THF:MCH 30:70, images with various sizes (wide view).

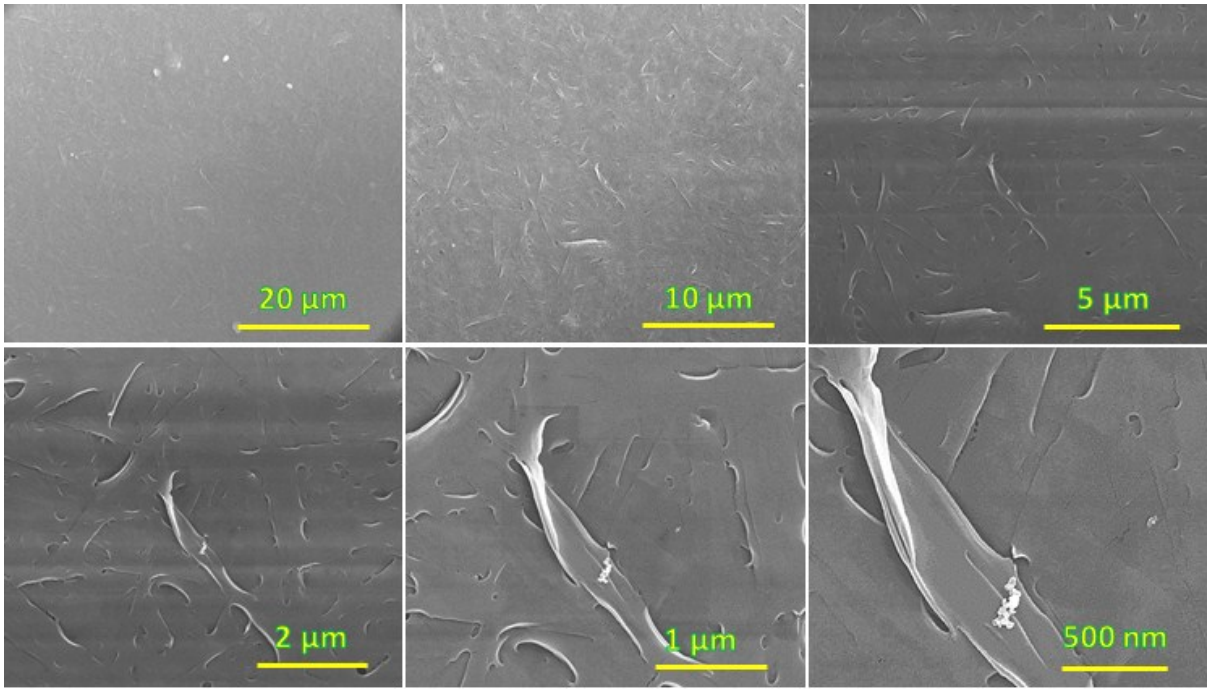

Fig. S16 SEM micrograph of NDI-TA2 self-assembled solid deposited from THF:MCH 30:70, images with various sizes 20 µm to 500 nm..

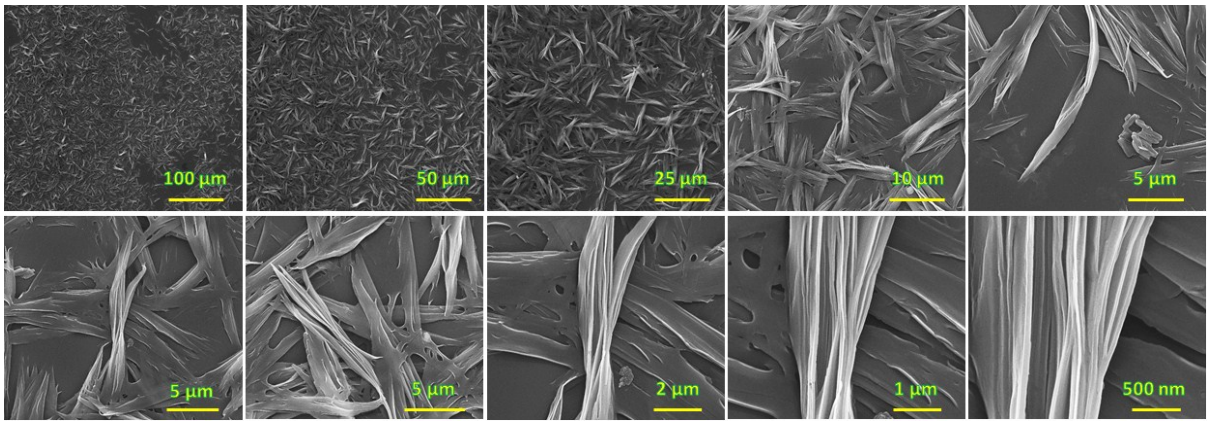

Fig. S17 SEM micrograph of NDI-TA2 self-assembled solid deposited from THF:MCH 10:90, images with various sizes 100 µm to 500 nm.

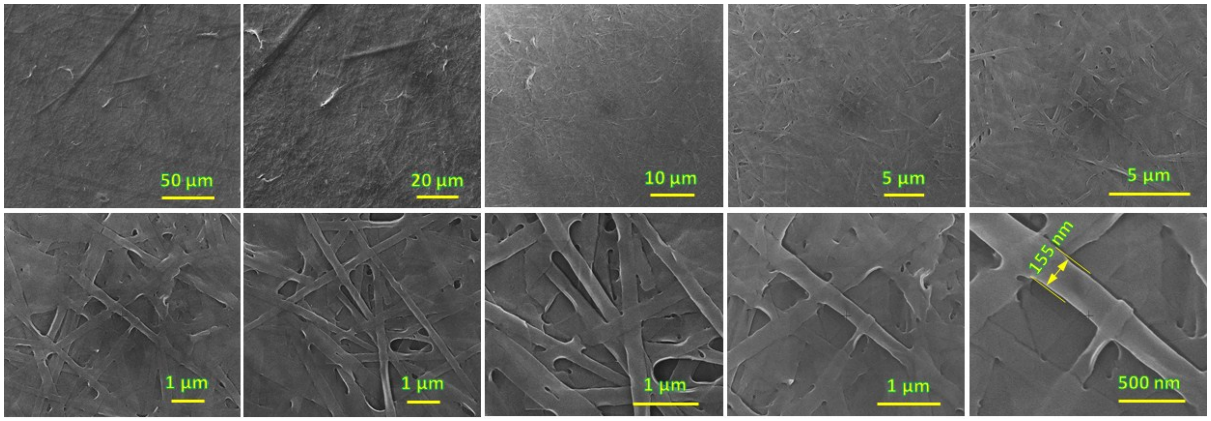

Fig. S18 SEM micrograph (wide view) of NDI-TA1 self-assembled solid deposited from THF:water 30:70 with varying image sizes 50 µm to 500 nm.

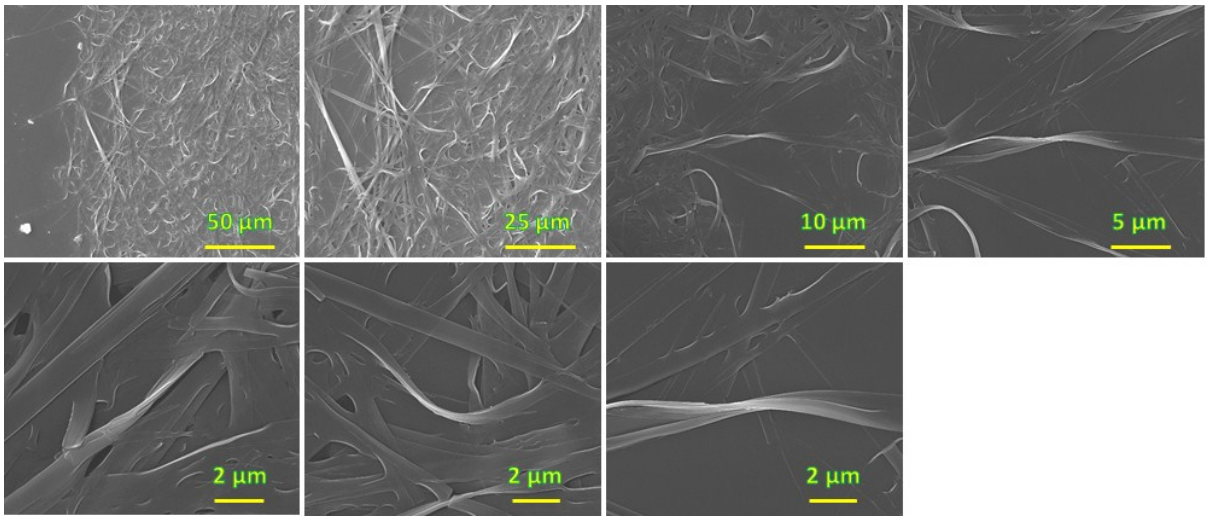

Fig. S19 SEM micrograph of NDI-TA2 self-assembled solid deposited from THF:water 30:70, images with various sizes 50 µm to 500 nm..

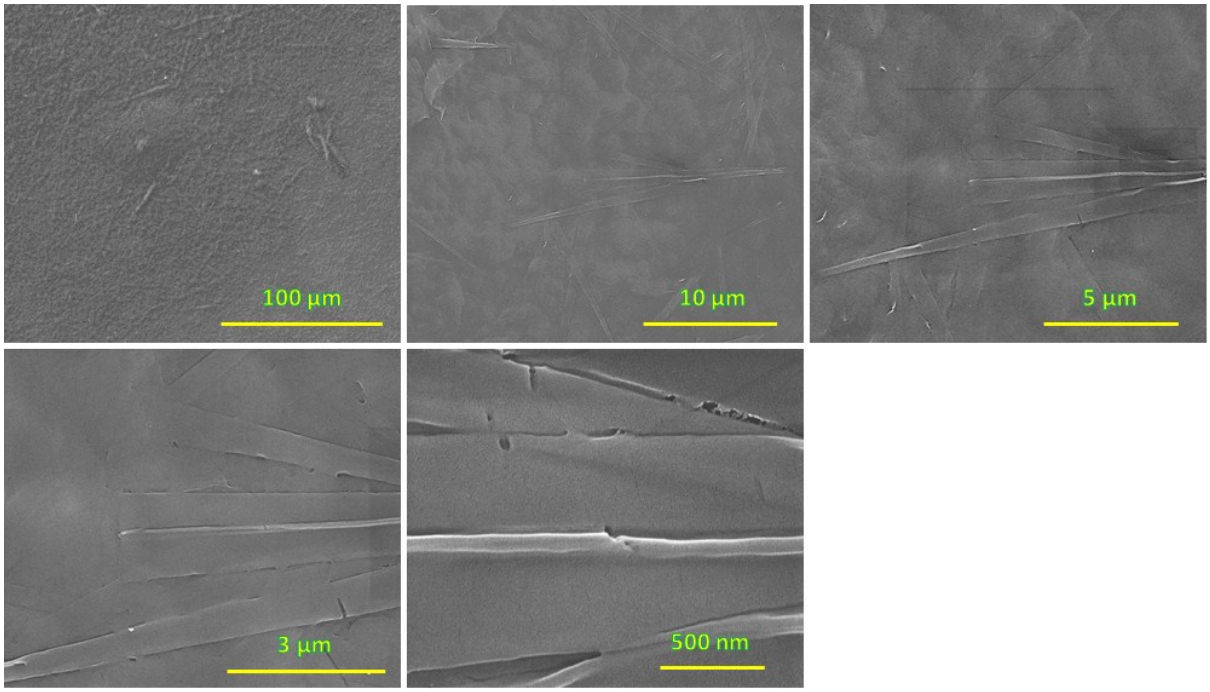

Fig. S20 SEM micrograph of NDI-TA1 (wide view) self-assembled solid deposited from THF:water 10:90 with varying image sizes 100 µm to 500 nm.

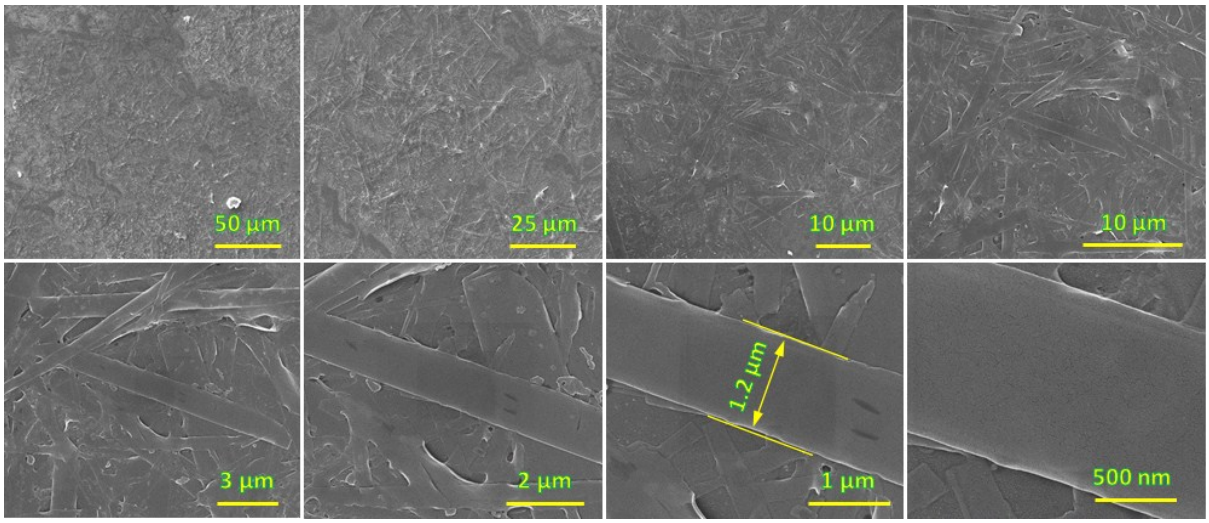

Fig. S21 SEM micrograph of NDI-TA2 self-assembled solid deposited from THF:water 10:90 (*v*/*v*), images with various sizes 50 µm to 500 nm.

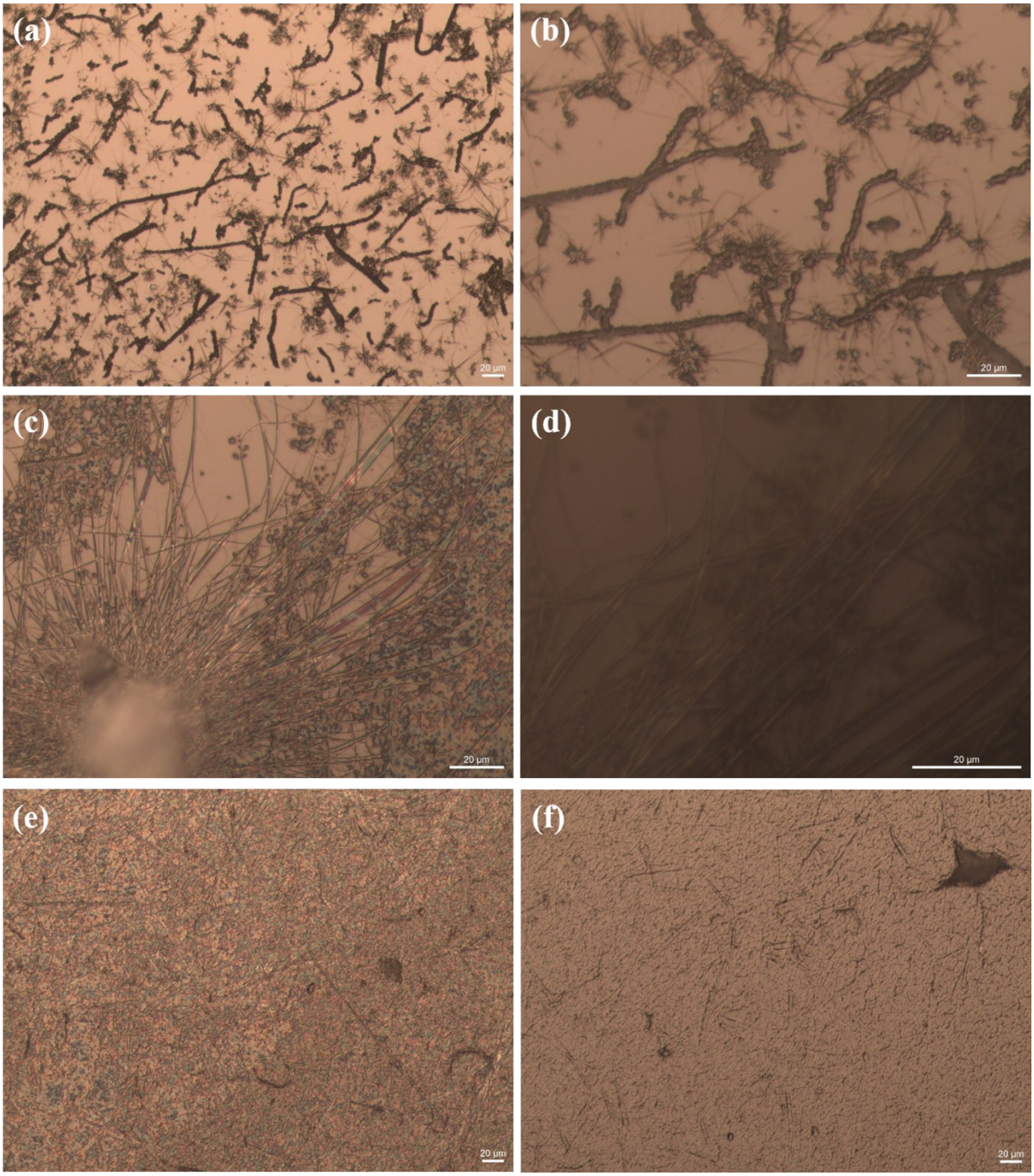

Fig. S22 POM images of NDI-TA1 from (a,b) THF:MCH (30:70, *v/v*); (c,d) THF:MCH (10:90, *v/v*); (e) THF:water (30:70, *v/v*) and (f) THF:water (10:90, *v/v*).

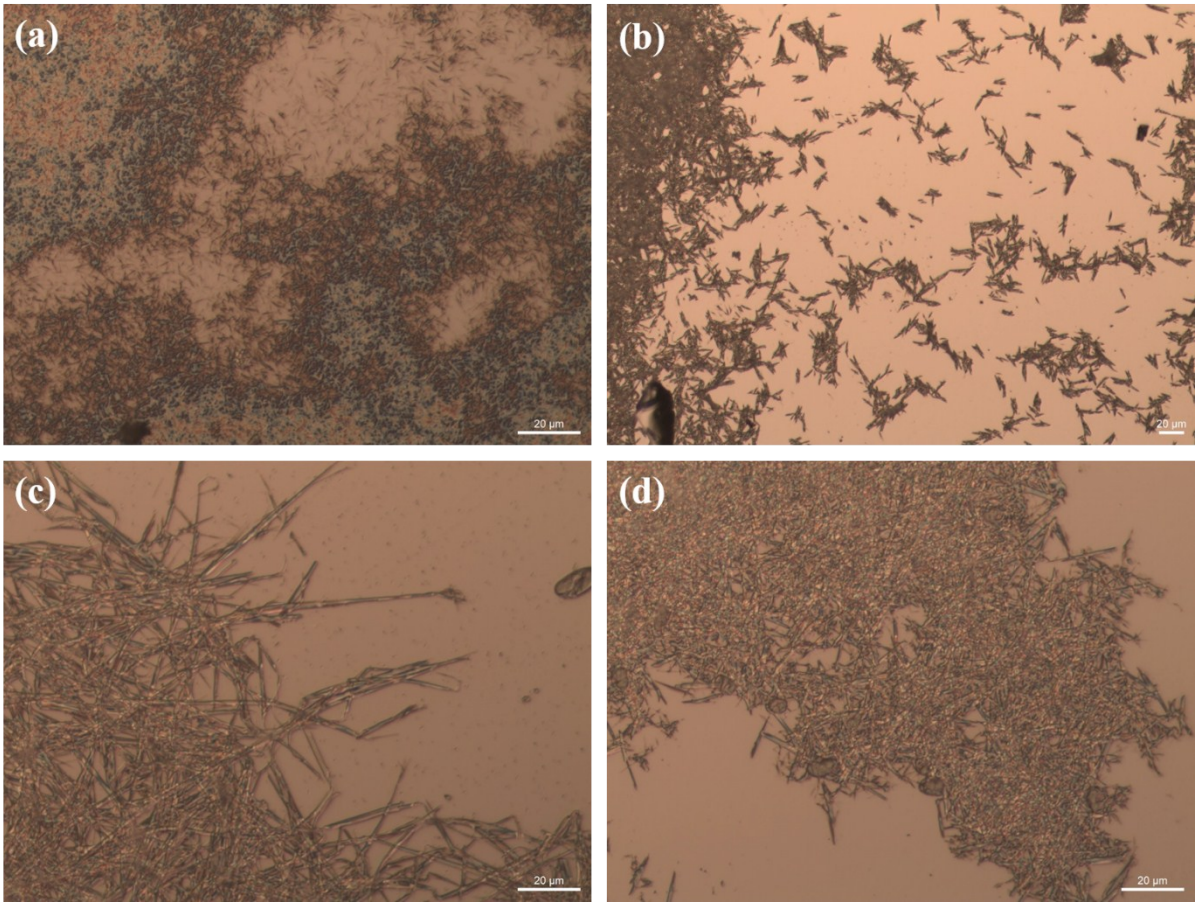

Fig. S23 POM images of NDI-TA2 from (a) THF:MCH (30:70, *v/v*); (b) THF:MCH (10:90, *v/v*); (c) THF:water (30:70, *v/v*) and (d) THF:water (10:90, *v/v*).

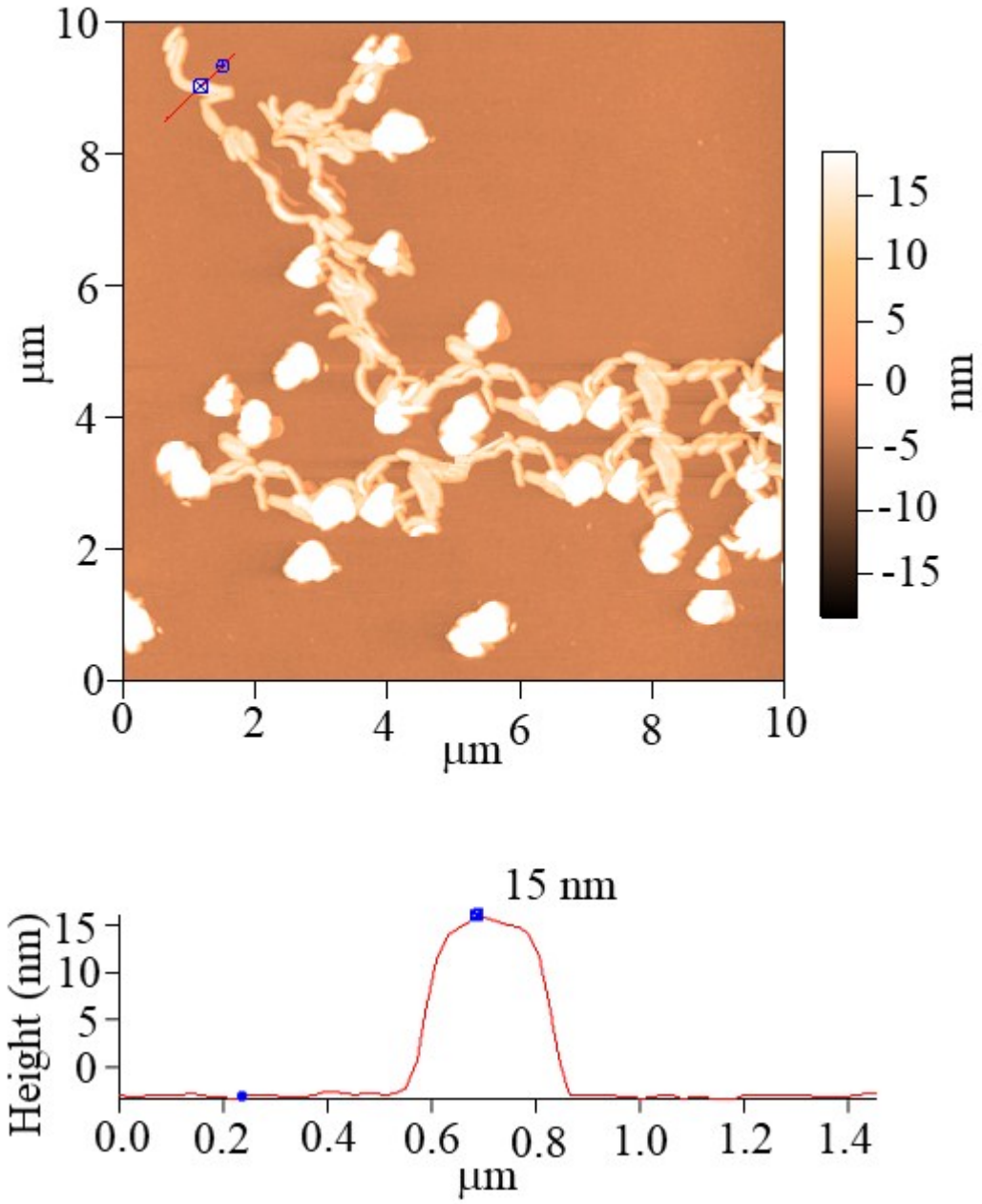

Fig. S24 AFM image of NDI-TA1 from THF:MCH (30:70, *v/v*).

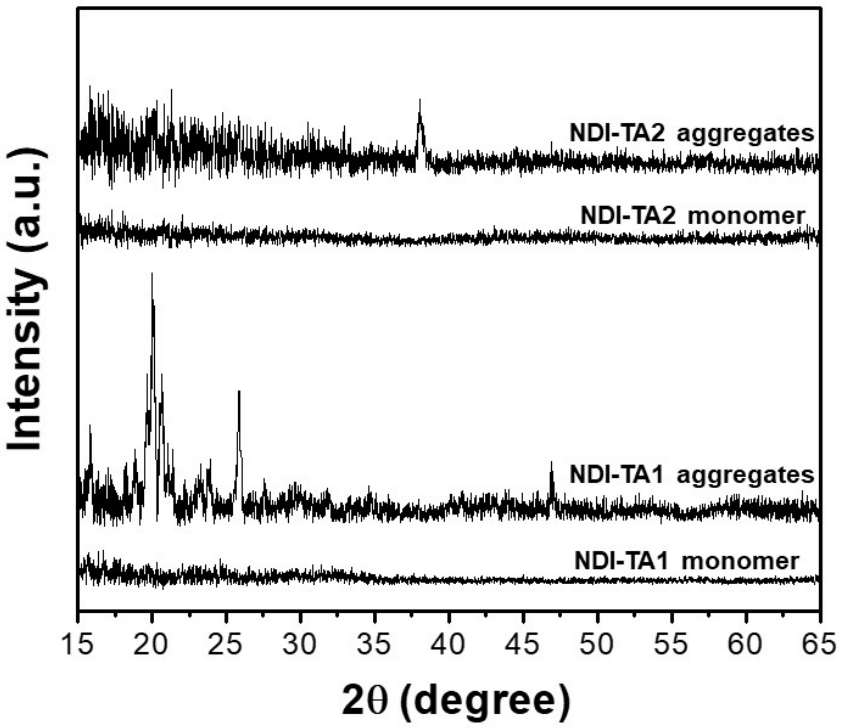

Fig. S25 XRD patterns of NDI-TA1 and NDI-TA2 monomer and self-assembled in THF/MCH (30:70, *v/v* ratio) mixtures.

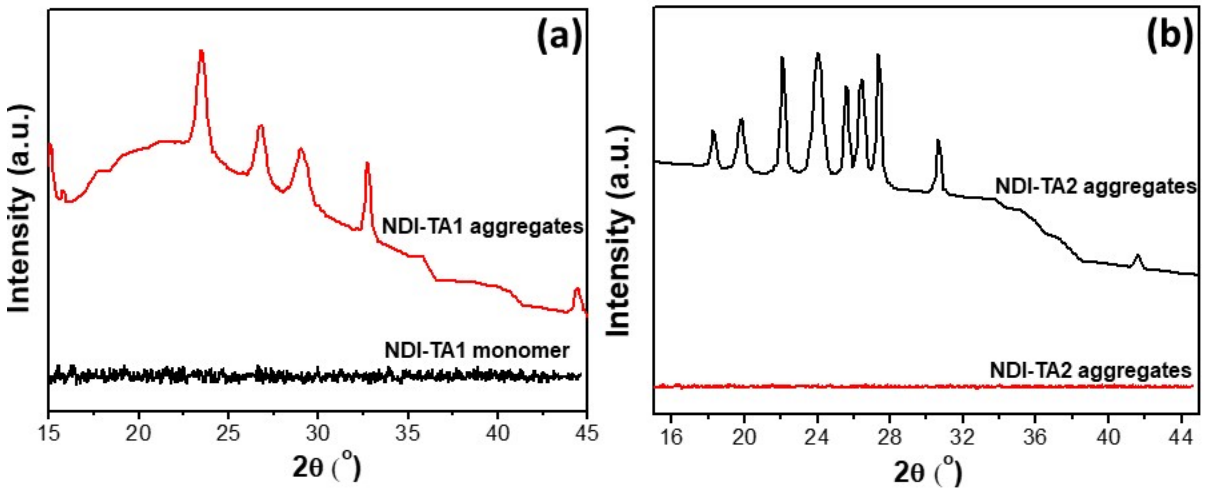

Fig. S26 XRD patterns of (a) NDI-TA1 monomer and self-assembled in THF/H_2O mixtures and (b) NDI-TA2 monomer and self-assembled in THF/H_2O (30:70, *v/v* ratio) mixtures.

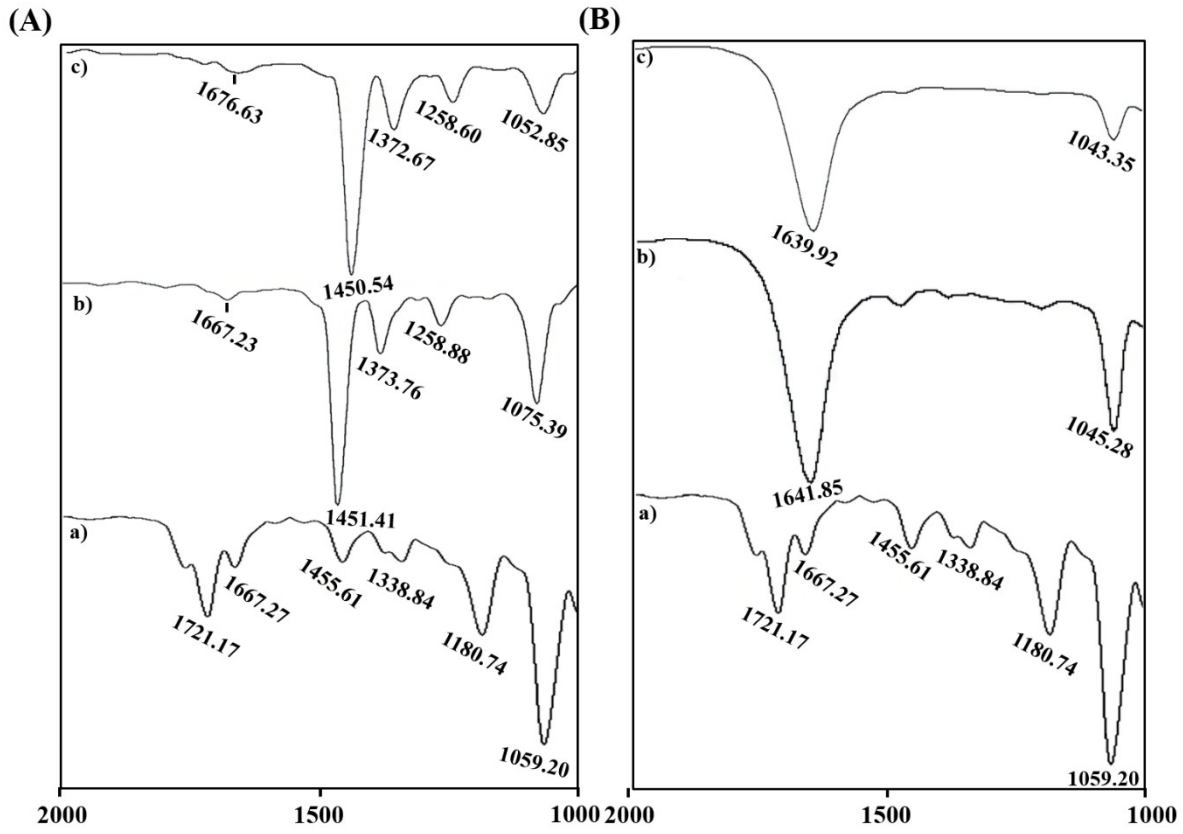

Fig. S27 FT-IR transmission spectra of NDI-TA1 in **(A)** (a) THF; (b) THF:MCH (30:70, *v/v*); (c) THF:MCH (10:90, *v/v*) and **(B)** (a) THF; (b) THF:H_2O (30:70, *v/v*); (c) THF:H_2O (10:90, *v/v*).

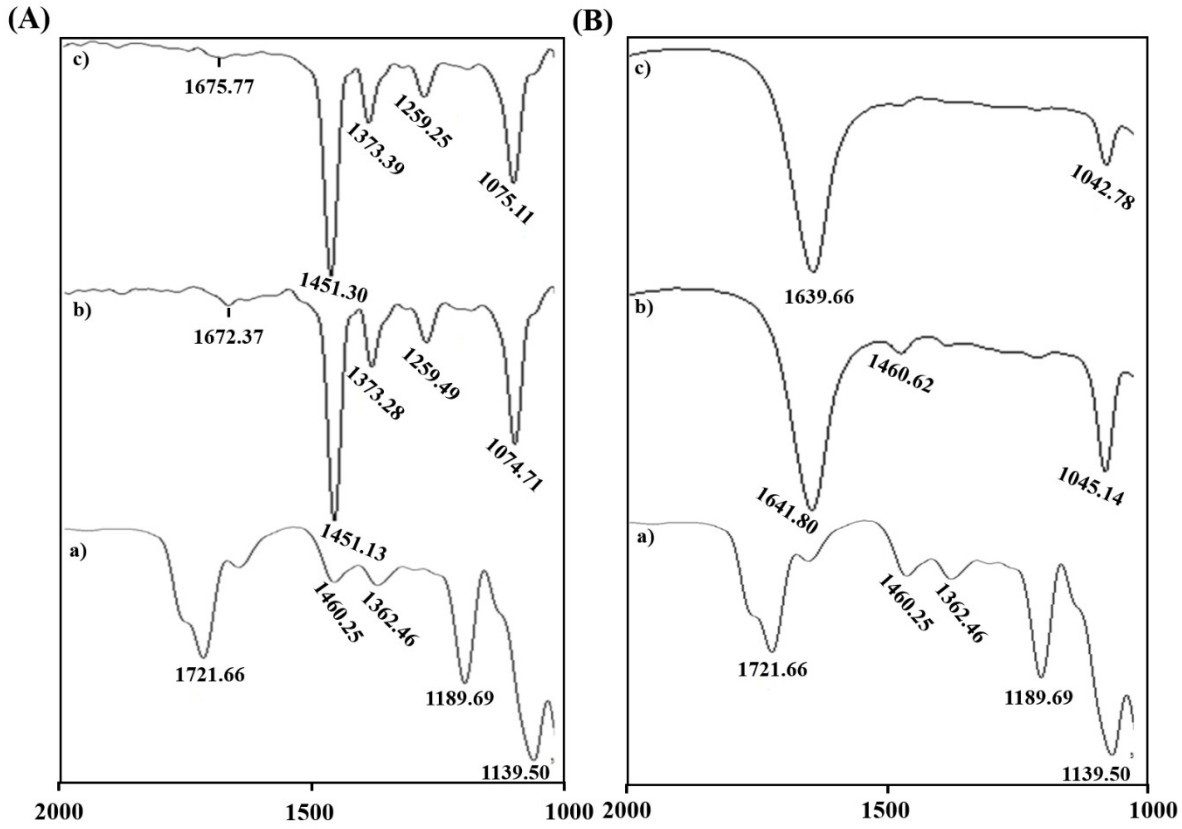

Fig. S28 FT-IR transmission spectra of NDI-TA2 in **(A)** (a) THF; (b) THF:MCH (30:70, *v/v*); (c) THF:MCH (10:90, *v/v*) and **(B)** (a) THF; (b) THF:H_2O (30:70, *v/v*); (c) THF:H_2O (10:90, *v/v*).

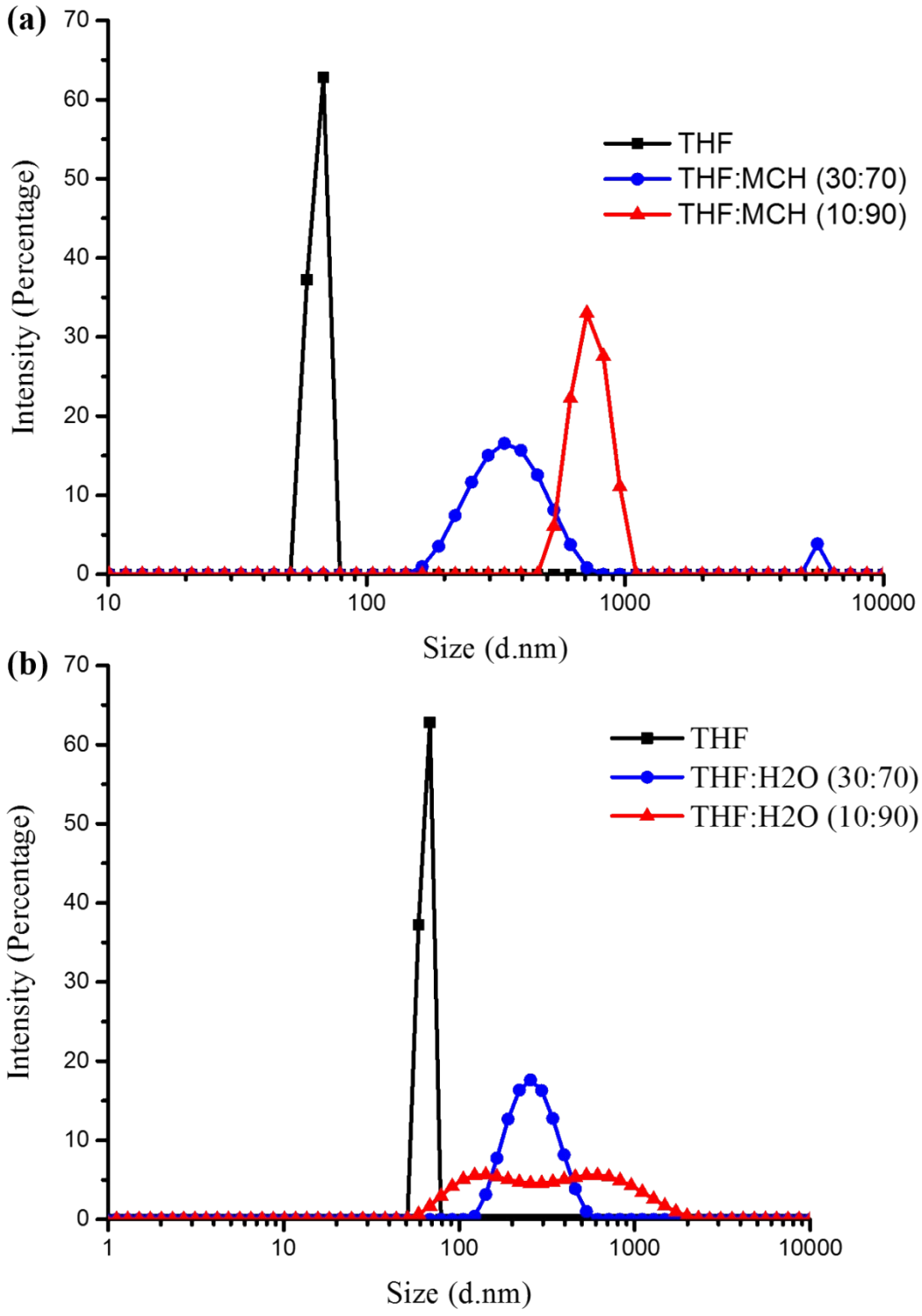

Fig. S29 The hydrodynamic diameter distribution of NDI-TA1 self-assembly growth by addition of MCH (a), and water (b) in THF as measured using dynamic light scattering (DLS) particle size analyser.

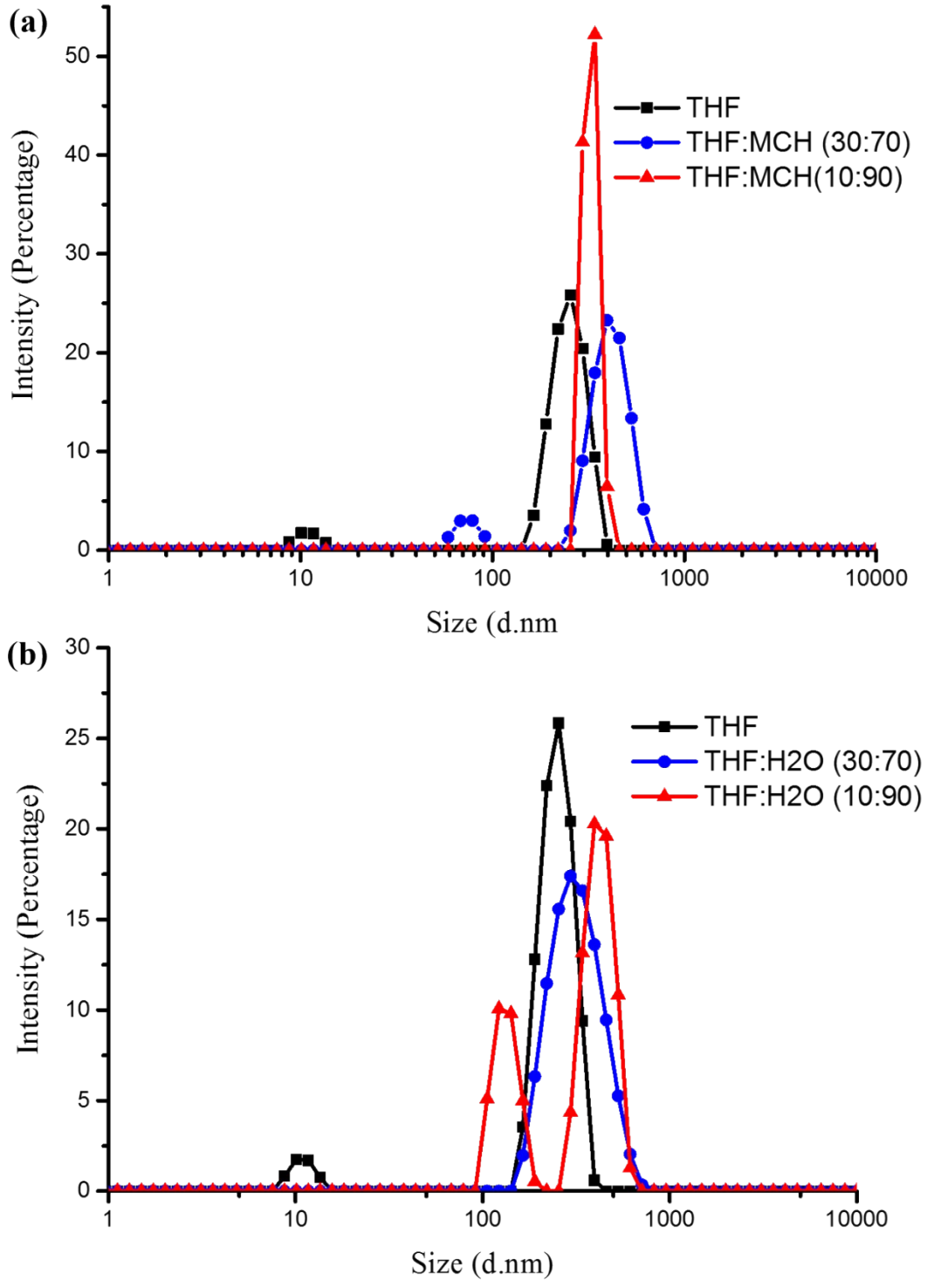

Fig. S30 The hydrodynamic diameter distribution of NDI-TA2 self-assembly growth by addition of MCH (a), and water (b) in THF as measured using dynamic light scattering (DLS) particle size analyser.

Molecular Modelling

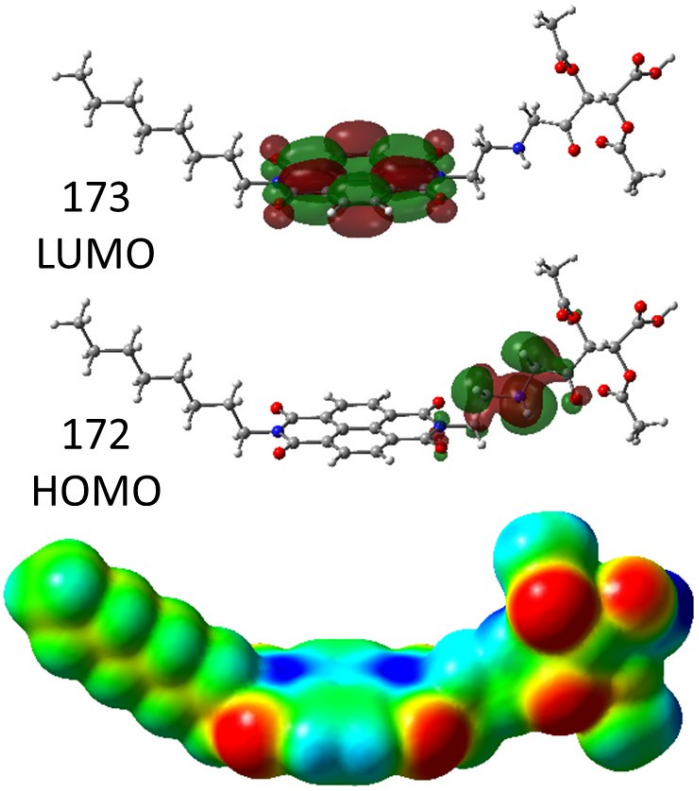

Fig. S31 The frontier molecular orbitals HOMO and LUMO wave function and total electron density of NDI-TA1 as calculated using TDDFT at B3LYP/6-311+G(d,p) level of theory and Gauss-Sum 3.0 program.

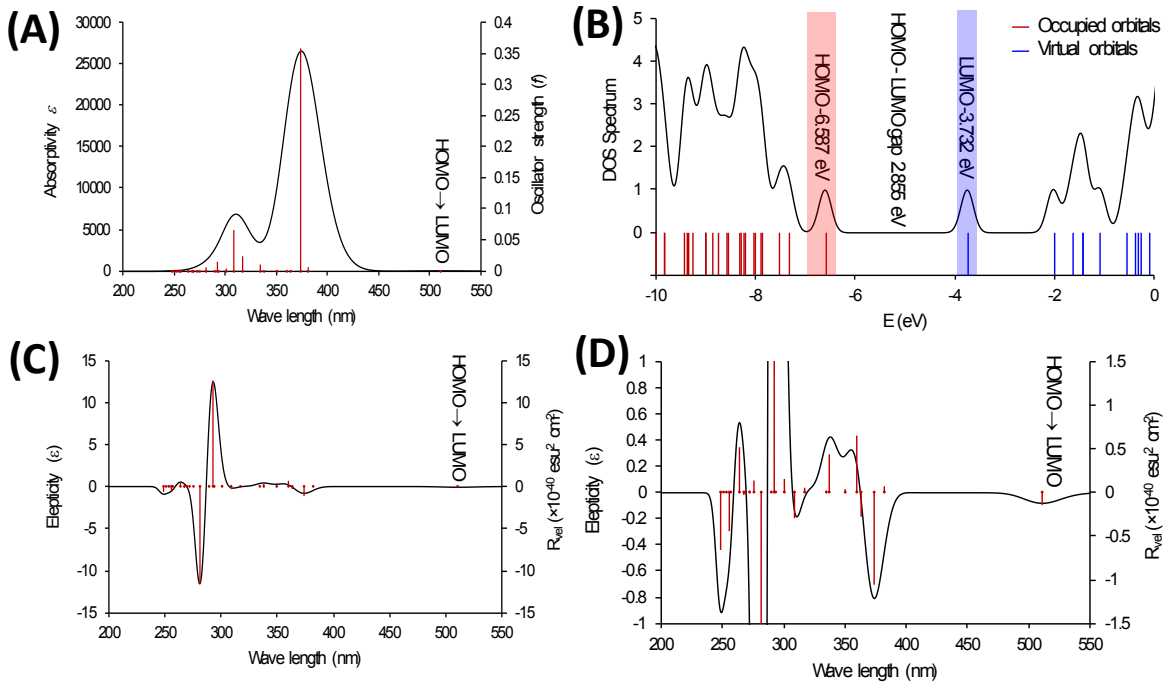

Fig. S32 The UV-vis (A), (B) density of state (DOS), and (C and D) cyclic dichroism (CD) spectra of NDI-TA1 as calculated using TDDFT at B3LYP/6-311+G(d,p) level of theory and Gauss-Sum 3.0 program.